Nonlinear Dyn
https://doi.org/10.1007/s11071-020-06112-5

ORIGINAL PAPER

Rogue wave solutions and the bright and dark solitons of the (3+1)-dimensional Jimbo–Miwa equation

Run-Fa Zhang · Ming-Chu Li · Hui-Min Yin

Received: 12 October 2020 / Accepted: 20 November 2020

Abstract It is well known that most classical test functions to solve nonlinear partial differential equations can be constructed via single hidden layer neural network model by using Bilinear Neural Network Method (BNNM). In this paper, the neural network model of test function for the (3+1)-dimensional Jimbo–Miwa equation is extended to the "4-2-3" model. By giving some specific activation functions, new test function is constructed to obtain analytical solutions of the (3+1)-dimensional Jimbo–Miwa equation. Rogue wave solutions and the bright and dark solitons are obtained by giving some specific parameters. Via curve plots, three-dimensional plots, contour plots and density plots, dynamical characteristics of these waves are exhibited.

Keywords Bilinear neural network method · Rogue wave · Bright and dark solitons · (3+1)-dimensional Jimbo–Miwa equation

R-F. Zhang (✉) · M-C. Li (✉)
School of Software Technology, Dalian University of Technology, Dalian 116620, China
e-mail: zhangrf@mail.dlut.edu.cn

M-C. Li
e-mail: mingchul@dlut.edu.cn

H-M. Yin
Department of Mechanical Engineering, University of Hong Kong, Pok Fu Lam, Hong Kong, China
e-mail: hmy63110@126.com

1 Introduction

As is known to all, the dynamic characteristics and space structure of nonlinear phenomena can be studied by means of nonlinear evolution equations (NLEEs) [1–9]. Researchers have studied the limit form solution with some new method [10–12]. Due to the strong nonlinear characteristics of neural network model, researchers have payed attentions to the application of neural network model to solve NLEEs. The Bilinear Neural Network Method (BNNM) [13] is a newest method for getting the analytical symbolic solution of NLEEs via neural network model and corresponding tensor formulas. Most classical test functions for solving nonlinear partial differential equations, such as rogue wave solutions [14–17], interactions [18–21], soliton solution [22–25], lump solutions [26], lump-type solutions [27–30], breather solutions [31], M-lump solutions [32], solitary waves [33] and periodic wave solutions [34], can be constructed via single hidden layer neural network model by using BNNM. Because the deep neural network model has strong nonlinear characteristics, the test function constructed by the deep hidden layer neural network model can fit the original function of the NLEEs, rather than the test function constructed by the classical single hidden layer network model. So far, there is no research on the use of "4-2-3" neural network model concerning the (3+1)-dimensional Jimbo–Miwa equation.

In this paper, we break through the classical construction method of using single hidden layer neural network model to construct test function and study the following (3+1)-dimensional Jimbo–Miwa equation [35]:

$$u_{xxxy} + 3u_y u_{xx} + 3u_x u_{xy} + 2u_{yt} - 3u_{xz} = 0. \quad (1)$$

This equation is the second equation in the well-known KP-hierarchy of integrable systems, which is used to describe certain interesting (3+1)-dimensional nonlinear waves in fluid mechanics and physics. Based on Hirota bilinear method, interaction solutions for a reduced extended (3+1)-dimensional Jimbo–Miwa equation have been constructed by Wang et al. [36]. Interaction phenomena and the periodic lump waves of Eq. (1) have been studied by Zhang et al. [37]. Solitary-wave and new exact solutions for an extended (3+1)-dimensional Jimbo–Miwa-like equation have been constructed by Qi et al. [38]. High-order lumps, high-order breathers and hybrid solutions for an extended (3+1)-dimensional Jimbo–Miwa equation have been derived by Guo et al. [39]. Kuo et al. [40] have studied the resonant multi-soliton solutions to new (3+1)-dimensional Jimbo–Miwa equations by applying the linear superposition principle. Liu et al. [41] have studied the dynamics for different classes of interactive lump solutions for the 3D-Jimbo–Miwa model with some nonzero determinant conditions.

This paper is organized as follows. Section 2 will present the detailed steps of BNNM and the corresponding tensor formula will be proposed to obtain the analytical solutions of nonlinear PDEs. In Sect. 3, rogue wave solutions and the bright and dark solitons of Eq. (1) will be obtained via "4-2-3" neural network model. The dynamical characteristics of these waves are exhibited via curve plots, three-dimensional plots, contour plots and density plots. Section 4 will conclude this paper.

2 BNNM and its corresponding tensor formula

2.1 Bilinear form

Hirota bilinear form of the (3+1)-dimensional Jimbo–Miwa Eq. (1),

$$\begin{aligned} \mathrm{B_{JM}}(\psi) &:= (D_{p,x}^3 D_{p,y} + 2D_{p,t} D_{p,y} \\ &\quad - 3D_{p,x} D_{p,y})\psi \cdot \psi \\ &= 2(\psi_{xxxy}\psi - \psi_y \psi_{xxx} - 3\psi_x \psi_{xxy} + 3\psi_{xx}\psi_{xy} \\ &\quad + 2\psi_{yt}\psi - 2\psi_y\psi_t - 3\psi_{xz}\psi + 3\psi_x\psi_z) = 0, \end{aligned} \quad (2)$$

can be obtain under dependent variable transformation:

$$u(x, y, z, t) = 2[\ln \psi(x, y, z, t)]_x, \quad (3)$$

where the generalized bilinear operators D are defined by [42]

$$\begin{aligned} & D_{p,x_1}^{n_1} \cdots D_{p,x_M}^{n_M} a \cdot b(x_1, \cdots, x_M) \\ & \quad = \prod_{i=1}^{M} \left(\frac{\partial}{\partial x_i} + \alpha \frac{\partial}{\partial x_i^{'}} \right)^{n_i} \\ & \quad a(x_1, \cdots, x_M) b(x_1^{'}, \ldots, x_M^{'}) \mid_{x'=x_1, \ldots, x'=x_M}, \end{aligned} \quad (4)$$

$n_1, \ldots, n_M$ are arbitrary non-negative integers, and for an integer m, the mth power of α is computed as follows,

$$(\alpha_p)^m = (-1)^{r(m)}, m \equiv r(m) \bmod p, 0 \leq r(m) < p, \quad (5)$$

and D is the Hirota bilinear operator in (2) with $p = 2$.

2.2 Neural network model and corresponding tensor formula

To search for the analytical solutions of the bilinear Eq. (2), the tensor formula of nonlinear neural network is constructed as following [13]:

$$\psi = w_{\boldsymbol{l_n},\psi} \phi_{\boldsymbol{l_n}}(\xi_{\boldsymbol{l_n}}), \quad (6)$$

where $w_{a,b}$ is the weight coefficient of neuron a to b, ϕ is a generalized activation function, which can be defined arbitrarily, but in the last layer, function ϕ must satisfy $\phi_{\boldsymbol{l_n}}(\xi) \geq 0$. $\boldsymbol{l_n} = \{m_{n-1}+1, m_{n-1}+2, \ldots, n\}$ represents the nth layer space of the neural network model. $\xi_{\boldsymbol{l_i}}$ is given as follows:

$$\xi_{\boldsymbol{l_i}} = w_{\boldsymbol{l_{i-1}},\boldsymbol{l_i}} \phi_{\boldsymbol{l_{i-1}}}(\xi_{\boldsymbol{l_{i-1}}}) + b_{\boldsymbol{l_i}}, \quad i = 1, 2, \ldots, n, \quad (7)$$

where $\boldsymbol{l_0} = \{x, y, \ldots, t\}$, $\boldsymbol{l_1} = \{1, 2, \ldots, m_1\}$, $\boldsymbol{l_i} = \{m_{i-1}+1, m_{i-1}+2, \ldots, m_i\}$, $(i = 2, 3, \ldots, n-1)$, b means a threshold, which can be simply understood here as an constant. This neural network tensor model can be intuitively understood through Fig. 1.

In order to obtain the analytical solutions of nonlinear PDEs, we take its main steps as follows:

Step 1: Through the bilinear transformation (3), the original Eq. (1) is transformed into the bilinear Eq. (2).

Step 2: Substituting Eq. (6) into the bilinear Eq. (2), a complicated equation can be obtained.

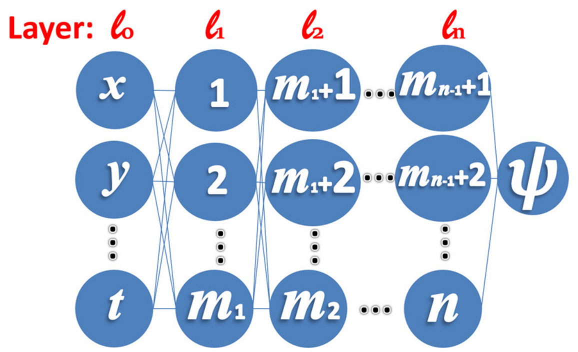

Fig. 1 Neural network model of Eq. (6): $\boldsymbol{l_0} = \{x, y, \ldots, t\}$, $\boldsymbol{l_1} = \{\xi_1, \xi_2, \ldots, \xi_{m_1}\}$, $\boldsymbol{l_i}$=$\{\xi_{m_{i-1}+1}, \xi_{m_{i-1}+2}, \ldots, \xi_{m_i}\}$, $(i = 2, 3, \ldots, n-1)$. $\boldsymbol{l_n}$=$\{\xi_{m_{n-1}+1}, \xi_{m_{n-1}+2}, \ldots, \xi_n\}$

Step 3: Making the coefficient of each term in this complicated equation equal to zero, we can obtain the overdetermined nonlinear algebraic equations.

Step 4: Solving these set of algebraic equations by symbolic computation with the help of Maple (or Mathematica), the coefficient solutions can be obtained.

Step 5: Substituting these coefficient solutions and nonlinear neural network tensor formula Eq. (6) into bilinear transformation Eq. (3), the analytical solutions of nonlinear PDEs can be derived.

Step 6: By choosing appropriate values and functions of these parameters in the analytical solutions of nonlinear PDEs, the dynamical characteristics of these solutions can be exhibited via three-dimensional plots, contour plots and density plots with the help of Maple (or Mathematica).

3 Rogue wave solutions and the bright and dark solitons

To search for the analytical solutions of Eq. (1), we can chose a "4-2-3" neural network model, which means that there are 4 neurons in the input layer $\boldsymbol{l_0}$, 2 neurons in hidden layer $\boldsymbol{l_1}$ and 3 neurons in hidden layer $\boldsymbol{l_2}$. This "4-2-3" model can be intuitively understood through Fig. 2. By choosing $\boldsymbol{l_0}$=$\{x, y, z, t\}$, $\boldsymbol{l_1}$=$\{1, 2\}$, $\boldsymbol{l_2}$=$\{3, 4, 5\}$, $\phi_1(\xi_1) = \cos(\xi_1), \phi_2(\xi_2) = \sin(\xi_2), \phi_3(\xi_3) = \exp(\xi_3), \phi_4(\xi_4) = \exp(\xi_4), \phi_5(\xi_5) = {\xi_5}^2$, we procure:

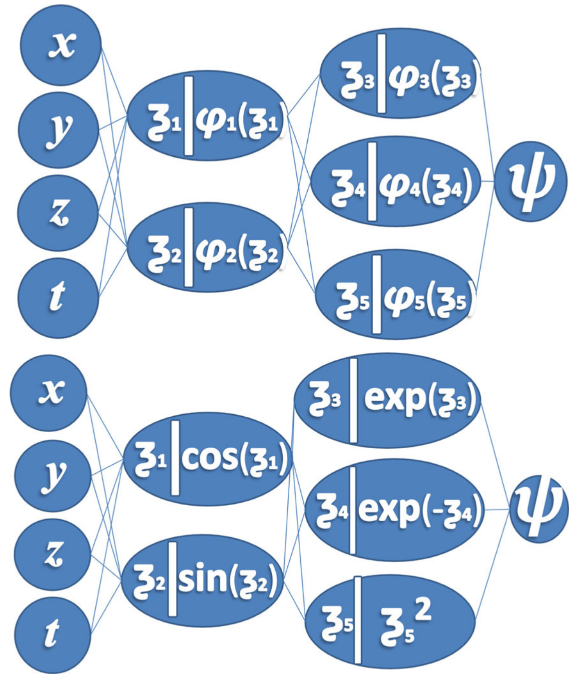

Fig. 2 "4-2-3" neural network model of Eq. (8) by choosing $\phi_1(\xi_1) = \cos(\xi_1), \phi_2(\xi_2) = \sin(\xi_2), \phi_3(\xi_3) = \exp(\xi_3), \phi_4(\xi_4) = \exp(-\xi_4), \phi_5(\xi_5) = {\xi_5}^2$

$$\psi = w_{3,\psi}\phi_3(\xi_3) + w_{4,\psi}\phi_4(\xi_4) + w_{5,\psi}\phi_5(\xi_5),$$
$$\begin{cases} \xi_3 = w_{1,3}\phi_1(\xi_1) + w_{2,3}\phi_2(\xi_2) + b_3, \\ \xi_4 = w_{1,4}\phi_1(\xi_1) + w_{2,4}\phi_2(\xi_2) + b_4, \\ \xi_5 = w_{1,5}\phi_1(\xi_1) + w_{2,5}\phi_2(\xi_2) + b_5, \\ \xi_1 = w_{t,1}t + w_{x,1}x + w_{y,1}y + w_{z,1}z + b_1, \\ \xi_2 = w_{t,2}t + w_{x,2}x + w_{y,2}y + w_{z,2}z + b_2, \end{cases} \tag{8}$$

where $w_{i,j}$ $(i = x, y, z, t, 1, 2, 3, 4, 5, j = 1, 2, 3, 4, 5, \psi$ and $i \neq j)$ and b_k $(k = 1, 2, 3, 4, 5)$ are real parameters to be determined later.

Substituting Eq. (8) into Eq. (2), we obtain a complicated equation. Making the coefficient of each term in this equation equal to zero, we obtained 214 algebraic equations. Solving these algebraic equations by the symbolic computation with the help of Maple, we get 6 sets of solutions as follows:

$$\textbf{case1}: \{\mathbf{w_{1,3} = -w_{1,4}, w_{1,5} = 0, w_{2,5} = 0}, \\ w_{t,2} = 0, w_{x,2} = 0, w_{y,1} = 0, w_{z,1} = 0, b_5 = 0.\} \tag{9}$$

$$\textbf{case2}: \{\mathbf{w_{1,3} = -w_{1,4}, w_{1,5} = 0, w_{2,5} = 0, w_{t,1} = 0}, \\ w_{x,1} = 0, w_{y,2} = 0, w_{z,2} = 0, b_5 = 0.\} \tag{10}$$

$$\textbf{case3}: \{\mathbf{w_{1,5} = 0, w_{2,3} = -w_{2,4}, w_{2,5} = 0, w_{t,1} = 0},$$

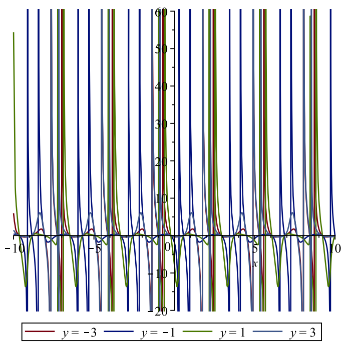

(a) x-curves

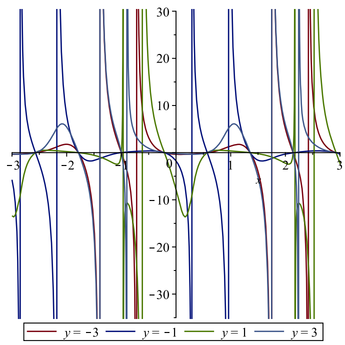

(b) x-curves

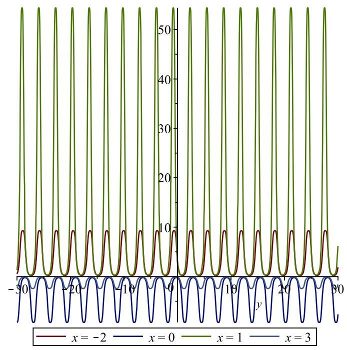

(c) y-curves

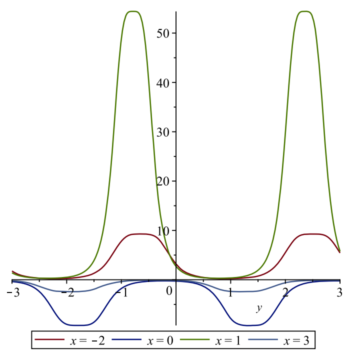

(d) y-curves

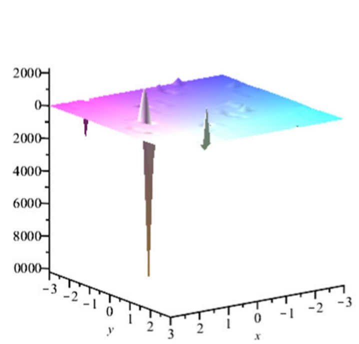

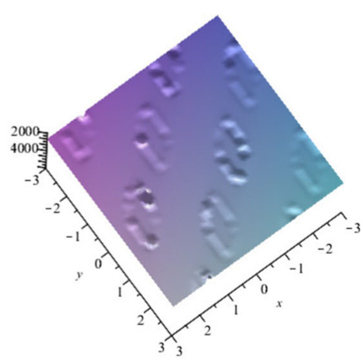

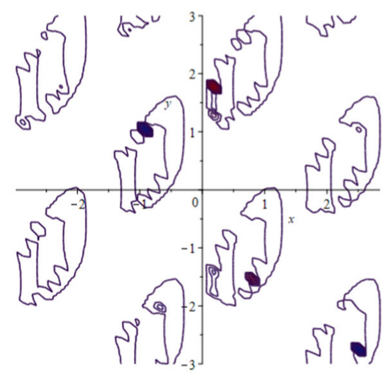

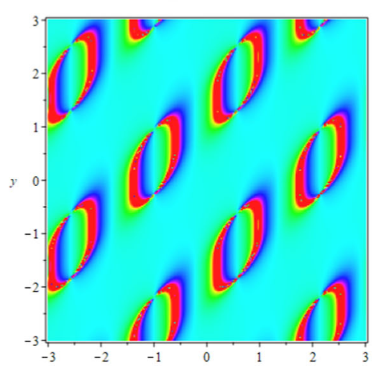

Fig. 3 (Color online) The curve plots, three-dimensional plots, contour plots and density plot of the rogue wave solutions for Eq. (15)

$$w_{x,1}=0,\, w_{y,2}=0,\, w_{z,2}=0,\, b_5=0.\} \tag{11}$$

$$\textbf{case4}:\{\mathbf{w_{1,5}=0,\, w_{2,3}=-w_{2,4},\, w_{2,5}=0,\, w_{t,2}=0},\; w_{x,2}=0,\, w_{y,1}=0,\, w_{z,1}=0,\, b_5=0.\} \tag{12}$$

$$\textbf{case5}:\{\mathbf{w_{1,3}=0,\, w_{1,4}}=0,\, w_{2,5}=0,\, w_{t,1}=\frac{w_{x,1}(4\,w_{x,1}{}^2 w_{y,2}+3\,w_{z,2})}{2w_{y,2}},\; w_{t,2}=0,\, w_{x,2}=0,\, w_{y,1}=0,\, w_{z,1}=0,\, b_5=0.\} \tag{13}$$

$$\textbf{case6}:\{\mathbf{w_{1,5}=0,\, w_{2,3}=0,\, w_{2,4}=0,\, w_{t,1}=0,\, w_{z,2}=0},\; w_{t,2}=\frac{w_{x,2}\left(4\,w_{x,2}{}^2 w_{y,1}+3\,w_{z,1}\right)}{2w_{y,1}},\, w_{x,1}=0,\, w_{y,2}=0,\, b_5=0.\} \tag{14}$$

Substituting (13) into Eq. (8), we can get the analytical solution for Eq. (1) through the bilinear transformation Eq. (3) when $w_{i,\psi}>0$ (i=3,4,5),

$$u=-4\,\frac{w_{5,\psi}w_{1,5}{}^2\cos(\xi_1)\,w_{x,1}\sin(\xi_1)}{\psi},$$
$$\begin{cases}\psi=w_{3,\psi}\mathrm{e}^{\xi_3}+w_{4,\psi}\mathrm{e}^{-w_{2,4}\sin(\xi_2)-b_4}\\ \quad +w_{5,\psi}w_{1,5}{}^2\left(\cos(\xi_1)\right)^2,\\ \xi_1=\frac{t w_{x,1}\left(4\,w_{x,1}{}^2 w_{y,2}+3\,w_{z,2}\right)}{2w_{y,2}}+x w_{x,1}+b_1,\\ \xi_2=y w_{y,2}+z w_{z,2}+b_2,\\ \xi_3=w_{2,3}\sin\left(y w_{y,2}+z w_{z,2}+b_2\right)+b_3.\end{cases} \tag{15}$$

In order to analyze the dynamics properties and discuss the evolution characteristic briefly, we could choose appropriate values and functions of these parameters in Eq. (15) as $z=x, t=0, w_{3,\psi}=1, w_{4,\psi}=1, w_{5,\psi}=-1, w_{1,5}=2, w_{x,1}=2, w_{y,2}=2, w_{z,2}=-2, w_{2,3}=2, w_{2,4}=2, b_3=2, b_4=2, b_1=2, b_2=2$. The evolution and dynamical characteristics of the rogue wave solutions derived via the appropriate values list above are exhibited in Fig. 3. Figure 3a and b shows the x-curve plots on the domain $(-10, 10)$ and $(-3, 3)$, respectively, from which we can find the exponential characteristics of Eq. (15). Figure 3c and d shows the y-curve plots on the domain $(-30, 30)$ and $(-3, 3)$, respectively, from which we can see the periodic characteristics of Eq. (15). Via three-dimensional plots, contour plots and density plots, we can find the rogue waves of Eq. (15), and dynamical characteristics of these waves are exhibited (Fig. 3).

In addition, we can construct new test functions by giving different activation functions, such as $\boldsymbol{l_0}=\{x, y, z, t\}$,

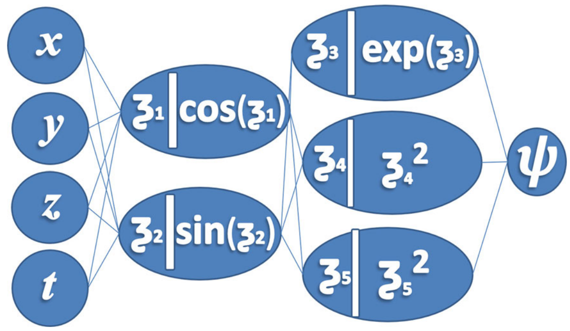

Fig. 4 "4-2-3" neural network model of Eq. (8) by choosing $\phi_1(\xi_1)=\cos(\xi_1), \phi_2(\xi_2)=\sin(\xi_2), \phi_3(\xi_3)=\exp(\xi_3), \phi_4(\xi_4)={\xi_5}^2, \phi_5(\xi_5)={\xi_5}^2$

$\boldsymbol{l_1}=\{1, 2\}$, $\boldsymbol{l_2}=\{3, 4, 5\}$, $\phi_1(\xi_1)=\cos(\xi_1), \phi_2(\xi_2)=\sin(\xi_2), \phi_3(\xi_3)=\exp(\xi_3), \phi_4(\xi_4)=\xi_4^2, \phi_5(\xi_5)={\xi_5}^2$, we procure:

$$\psi=w_{3,\psi}\mathrm{e}^{\xi_3}+w_{4,\psi}{\xi_4}^2+w_{5,\psi}{\xi_5}^2,$$
$$\begin{cases}\xi_3=w_{1,3}\cos(\xi_1)+w_{2,3}\sin(\xi_2)+b_3,\\ \xi_4=w_{1,4}\cos(\xi_1)+w_{2,4}\sin(\xi_2)+b_4,\\ \xi_5=w_{1,5}\cos(\xi_1)+w_{2,5}\sin(\xi_2)+b_5,\\ \xi_1=w_{t,1}t+w_{x,1}x+w_{y,1}y+w_{z,1}z+b_1,\\ \xi_2=w_{t,2}t+w_{x,2}x+w_{y,2}y+w_{z,2}z+b_2,\end{cases} \tag{16}$$

where $w_{i,j}$ $(i=x, y, z, t, 1, 2, 3, 4, 5, j=1, 2, 3, 4, 5, \psi$ and $i\neq j)$ and b_k $(k=1, 2, 3, 4, 5)$ are real parameters to be determined later. This test function can be intuitively understood through corresponding neural network model (Fig. 4).

Substituting Eq. (16) into Eq. (2), we obtain a complicated equation. Making the coefficient of each term in this equation equal to zero, we obtain 116 algebraic equations. Solving these algebraic equations by the symbolic computation with the help of Maple, we get 55 sets of solutions. One of the solutions is as follows,

$$\left\{\begin{array}{l} w_{1,3}=0,\, w_{5,\psi}=-\frac{w_{2,4}w_{1,4}w_{4,\psi}}{w_{1,5}w_{2,5}},\\ w_{t,2}=0,\, w_{x,2}=0,\, w_{y,1}=0,\\ w_{y,2}=\frac{3w_{x,1}w_{z,2}}{-4\,w_{x,1}{}^3+2w_{t,1}},\, w_{z,1}=0,\, b_4=\frac{b_5 w_{2,4}}{w_{2,5}}.\end{array}\right\} \tag{17}$$

Substituting (17) into Eq. (16), we can get the analytical solution for Eq. (1) through the bilinear transformation Eq. (3) when $w_{i,\psi}>0$ (i=3,4,5),

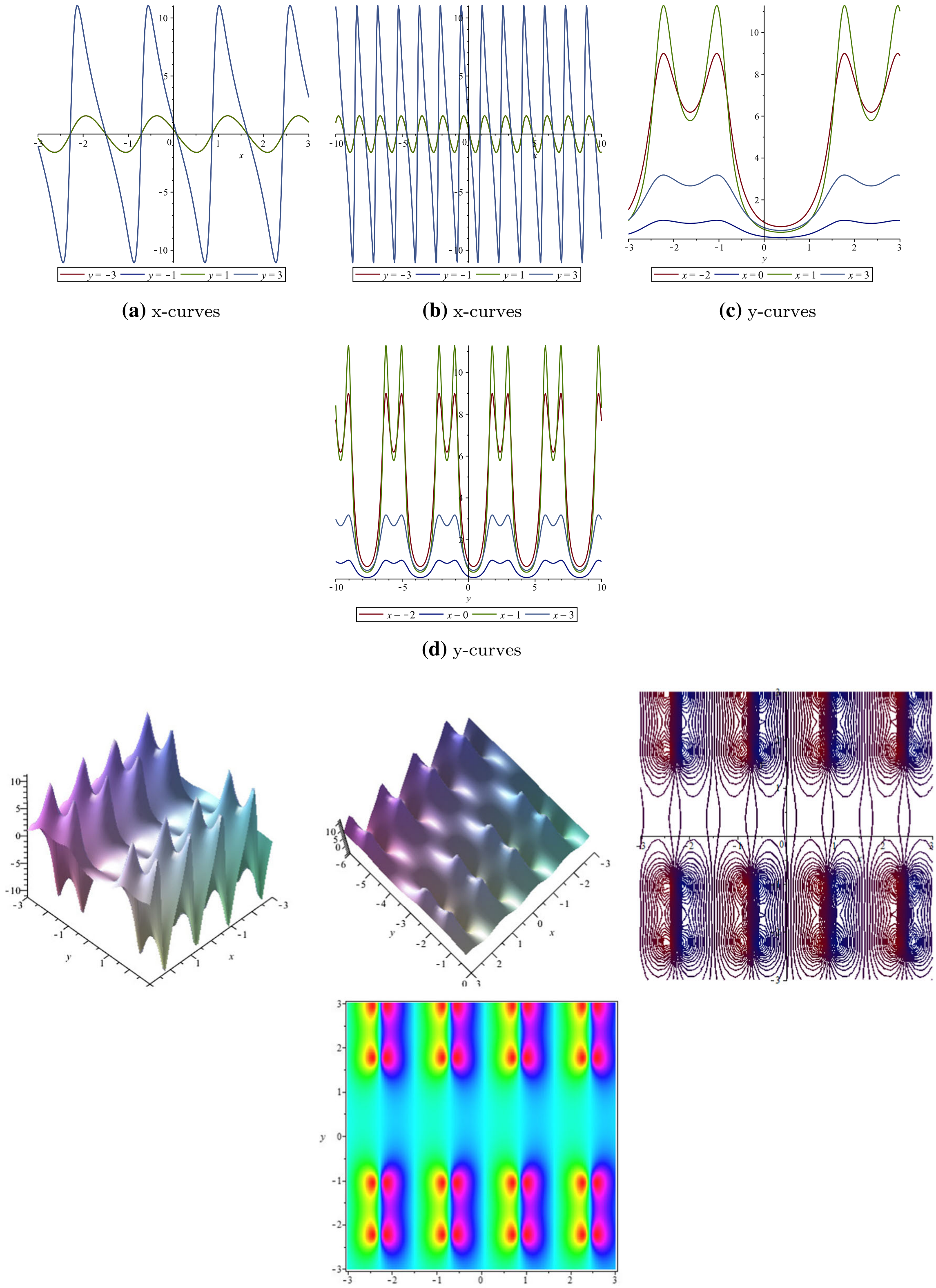

Fig. 5 (Color online) The curve plots, three-dimensional plots, contour plots and density plot of the bright and dark solitons for Eq. (18)

$$u = 4\frac{\sin(\xi_1)\, w_{1,4} w_{4,\psi} w_{x,1}\left(w_{2,4}\xi_5 - w_{2,5}\xi_4\right)}{\psi\, w_{2,5}},$$
$$\begin{cases} \psi = w_{3,\psi} e^{\xi_3} + w_{4,\psi}\xi_4{}^2 - \frac{w_{2,4}w_{1,4}w_{4,\psi}\xi_5{}^2}{w_{1,5}w_{2,5}}, \\ \xi_1 = t w_{t,1} + x w_{x,1} + b_1, \\ \xi_2 = \frac{3y w_{x,1} w_{z,2}}{-4\, w_{x,1}{}^3 + 2w_{t,1}} + z w_{z,2} + b_2, \\ \xi_3 = w_{2,3}\sin\left(\frac{3y w_{x,1} w_{z,2}}{-4\, w_{x,1}{}^3 + 2w_{t,1}} + z w_{z,2} + b_2\right) + b_3, \\ \xi_4 = w_{1,4}\cos(\xi_1) \\ +w_{2,4}\sin\left(\frac{3y w_{x,1} w_{z,2}}{-4\, w_{x,1}{}^3 + 2w_{t,1}} + z w_{z,2} + b_2\right) + \frac{b_5 w_{2,4}}{w_{2,5}}, \\ \xi_5 = w_{1,5}\cos(\xi_1) \\ +w_{2,5}\sin\left(\frac{3y w_{x,1} w_{z,2}}{-4\, w_{x,1}{}^3 + 2w_{t,1}} + z w_{z,2} + b_2\right) + b_5. \end{cases} \tag{18}$$

In order to analyze the dynamics properties and discuss the evolution characteristic briefly, we could choose appropriate values and functions of these parameters in Eq. (18) as $z = y, t = 1, w_{1,4} = 2, w_{1,5} = -2, w_{2,3} = 2, w_{2,4} = 2, w_{2,5} = 2, w_{x,1} = 2, w_{z,1} = 2, w_{t,1} = 2, w_{z,2} = 2, w_{3,\psi} = 2, w_{4,\psi} = 2, b_1 = 1, b_2 = 1, b_3 = 1, b_5 = 1$. The evolution and dynamic characteristics of the bright and dark solitons derived via the appropriate values list above are exhibited in Fig. 5. Figure 5a and b shows the x-curve plots on the domain $(-3, 3)$ and $(-10, 10)$, respectively, from which we can find the periodic characteristics of Eq. (15). Figure 5c and d shows the y-curve plots on the domain $(-3, 3)$ and $(-10, 10)$, respectively, from which we can see the exponential properties and periodic characteristics of Eq. (18). Via three-dimensional plots, contour plots and density plots, we can find the bright and dark solitons of Eq. (18), dynamical characteristics of these waves are exhibited.

In order to illustrate the reliability of the results (15) and (18), we substitute the results (15) and (18) into the left side of Eq. (1). With the help of automatic symbolic derivation software Maple, the simplification results show that the left side of Eq. (1) is equal to 0. It illustrates that analytical solutions (15) and (18) are reliable and accurate with zero error. It also shows the advantage of this method comparing the classical neural network method, which can only obtain approximate solutions. However, many numerical methods are generally applicable and effective, such as the structure-preserving method focusing on the local characteristics as well as the conservation laws of the systems [43–50].

4 Conclusions

The traditional neural network method for solving nonlinear partial differential equations is to discretize the function and then fit the original function with these discrete points to get the approximate solution. Different from this, we get the analytical solution for Eq. (1) by using Bilinear Neural Network Method (BNNM). The neural network model of test function for the (3+1)-dimensional Jimbo–Miwa equation is extended to the “4-2-3” model. By giving some specific activation functions, such as $\{\phi_1(\xi_1) = \cos(\xi_1), \phi_2(\xi_2) = \sin(\xi_2), \phi_3(\xi_3) = \exp(\xi_3), \phi_4(\xi_4) = \exp(\xi_4), \phi_5(\xi_5) = \xi_5{}^2\}$ or $\{\phi_1(\xi_1) = \cos(\xi_1), \phi_2(\xi_2) = \sin(\xi_2), \phi_3(\xi_3) = \exp(\xi_3), \phi_4(\xi_4) = \xi_5{}^2, \phi_5(\xi_5) = \xi_5{}^2\}$, new test function is constructed to obtain analytical solutions of Eq. (1). Giving some specific parameters, new rogue wave solutions and the bright and dark solitons are obtained. Via curve plots, three-dimensional plots, contour plots and density plots, dynamical characteristics of these waves are exhibited. That will be used to describe nonlinear phenomena in the fields of gas, plasma, optics, acoustics, heat transfer, fluid dynamics, classical mechanics and so on.

The neural network model can fit the nonlinear partial differential equations well because of its nonlinear properties. In the future, we can further optimize the neural network model to make it have more complex nonlinear characteristics, such as using “4-2-4” or “4-2-5” model to increase the breadth of the neural network, or using “4-2-3-2” or “4-2-3-2-2” model to increase the depth of the neural network model. In addition, we can directly use arbitrary functions $\phi(\xi_i)$ to calculate to obtain arbitrary function solutions for the (3+1)-dimensional Jimbo–Miwa equation. However, with the increase in the complexity of the neural network model, the amount of calculation becomes quite large, and the calculation time becomes particularly long. In the future, we can solve this bottleneck problem by parallel computing and quantum computing.

Acknowledgements This work is supported by the National Natural Science Foundation of China under Grant Nos.: 61572095 and 61877007.

Compliance with ethical standards

Conflict of interest The authors declare that they have no conflict of interest concerning the publication of this manuscript.

References

1. Wazwaz, A.M., Kaur, L.: New integrable Boussinesq equations of distinct dimensions with diverse variety of soliton solutions. Nonlinear Dyn. **97**, 83–94 (2019)
2. Xu, G.Q., Wazwaz, A.M.: Bidirectional solitons and interaction solutions for a new integrable fifth-order nonlinear equation with temporal and spatial dispersion. Nonlinear Dyn. **101**, 581–595 (2020)
3. Wazwaz, A.M.: Two new integrable fourth-order nonlinear equations: multiple soliton solutions and multiple complex soliton solutions. Nonlinear Dyn. **94**, 2655–2663 (2018)
4. Lan, Z.Z., Hu, W.Q., Guo, B.L.: General propagation lattice Boltzmann model for a variable-coefficient compound KdV-Burgers equation. Appl. Math. Modell. **73**, 695–714 (2019)
5. Xu, G.Q., Wazwaz, A.M.: Integrability aspects and localized wave solutions for a new (4+1)-dimensional Boiti–Leon–Manna–Pempinelli equation. Nonlinear Dyn. **98**, 1379–1390 (2019)
6. Osman, M.S., Wazwaz, A.M.: An efficient algorithm to construct multi-soliton rational solutions of the (2+ 1)-dimensional KdV equation with variable coefficients. Appl. Math. Comput. **321**, 282–289 (2018)
7. Wazwaz, A.M., Xu, G.Q.: Kadomtsev-petviashvili hierarchy: two integrable equations with time-dependent coefficients. Nonlinear Dyn. **100**, 3711–3716 (2020)
8. Lan, Z.Z., Guo, B.L.: Nonlinear waves behaviors for a coupled generalized nonlinear Schrödinger–Boussinesq system in a homogeneous magnetized plasma. Nonlinear Dyn. **100**, 3771–3784 (2020)
9. McAnally, M., Ma, W.X.: An integrable generalization of the D-Kaup-Newell soliton hierarchy and its bi-Hamiltonian reduced hierarchy. Appl. Math. Comput. **323**, 220–227 (2018)
10. Hu, B.B., Zhang, L., Xia, T.C., Zhang, N.: On the riemann-hilbert problem of the kundu equation. Appl. Math. Comput. **381**, 125262 (2020)
11. Hu, B.B., Xia, T.C., Ma, W.X.: Riemann-hilbert approach for an initial-boundary value problem of the two-component modified korteweg-de vries equation on the half-line. Appl. Math. Comput. **332**, 148–159 (2018)
12. Hu, B.B., Cheng Xia, T., Zhang, N., Bo Wang, J.: Initial-boundary value problems for the coupled higher-order nonlinear schrödinger equations on the half-line. Int. J. Nonlinear Sci. Num. **19**(1), 83–92 (2018)
13. Zhang, R.F., Bilige, S.D.: Bilinear neural network method to obtain the exact analytical solutions of nonlinear partial differential equations and its application to p-gBKP equatuon. Nonlinear Dyn. **95**, 3041–3048 (2019)
14. Lan, Z.Z., Su, J.J.: Solitary and rogue waves with controllable backgrounds for the non-autonomous generalized AB system. Nonlinear Dyn. **96**, 2535–2546 (2019)
15. Yin, H.M., Tian, B., Zhao, X.C., Zhang, C.R., Hu, C.C.: Breather-like solitons, rogue waves, quasi-periodic/chaotic states for the surface elevation of water waves. Nonlinear Dyn. **97**, 21–31 (2019)
16. Lan, Z.Z.: Rogue wave solutions for a higher-order nonlinear Schrödinger equation in an optical fiber. Appl. Math. Lett. **107**, 106382 (2020)
17. Yin, H.M., Tian, B., Zhang, C.R., Du, X.X., Zhao, X.C.: Optical breathers and rogue waves via the modulation instability for a higher-order generalized nonlinear Schrödinger equation in an optical fiber transmission system. Nonlinear Dyn. **97**, 843–852 (2019)
18. Ma, W.X., Yong, X.L., Zhang, H.Q.: Diversity of interaction solutions to the (2+1)-dimensional Ito equation. Comput. Math. Appl. **75**, 289–295 (2018)
19. Ma, W.X.: Lump and interaction solutions to linear (4+1)-dimensional PDEs. Acta Math. Sci. **39B**(2), 498–508 (2019)
20. Hua, Y.F., Guo, B.L., Ma, W.X., Lü, X.: Interaction behavior associated with a generalized (2+1)-dimensional Hirota bilinear equation for nonlinear waves. Appl. Math. Modell. **74**, 184–198 (2019)
21. Liu, J.G.: Lump-type solutions and interaction solutions for the (2+1)-dimensional asymmetrical Nizhnik-Novikov-Veselov equation. Eur. Phys. J. Plus **134**, 56 (2019)
22. Lan, Z.Z.: Multi-soliton solutions for a (2+1)-dimensional variable-coefficient nonlinear schrödinger equation. Appl. Math. Lett. **86**, 243–248 (2018)
23. Wazwaz, A.M., Kaur, L.: Complex simplified hirota's forms and lie symmetry analysis for multiple real and complex soliton solutions of the modified KdV-Sine-Gordon equation. Nonlinear Dyn. **95**, 2209–2215 (2019)
24. Lan, Z.Z.: Soliton and breather solutions for a fifth-order variable-coefficient nonlinear Schrödinger equation in an optical fiber. Appl. Math. Lett. **102**, 106132 (2020)
25. Osman, M.S.: One-soliton shaping and inelastic collision between double solitons in the fifth-order variable-coefficient Sawada-Kotera equation. Nonlinear Dyn. **96**, 1491–1496 (2019)
26. Ma, W.X.: Bilinear equations, Bell polynomials and linear superposition principle. J. Phys. Conf. Ser. **411**, 012021 (2013)
27. Gai, L.T., Ma, W.X., Li, M.C.: Lump-type solution and breather lump-kink interaction phenomena to a (3+1)-dimensional GBK equation based on trilinear form. Nonlinear Dyn. **100**, 2715–2727 (2020)
28. Liu, J.G.: Lump-type solutions and interaction solutions for the (2+1)-dimensional generalized fifth-order KdV equation. Appl. Math. Lett. **86**, 36–41 (2018)
29. Gai, L.T., Ma, W.X., Li, M.C.: Lump-type solutions, rogue wave type solutions and periodic lump-stripe interaction phenomena to a (3+1)-dimensional generalized breaking soliton equation. Phys. Lett. A **384**, 126178 (2020)
30. Liu, J.G., Zhu, W.H.: Various exact analytical solutions of a variable-coefficient Kadomtsev-Petviashvili equation. Nonlinear Dyn. **100**, 2739–2751(2020)
31. Liu, W., Wazwaz, A.M., Zhang, X.X.: High-order breathers, lumps, and semirational solutions to the (2+1)-dimensional Hirota–Satsuma–Ito equation. Phys. Scr. **94**, 075203 (2019)
32. Zhang, X.E., Chen, Y.: M-lump, high-order breather solutions and interaction dynamics of a generalized (2+1)-dimensional nonlinear wave equation. Nonlinear Dyn. **100**, 2753–2765 (2020)
33. Ghanbari, B., Mustafa, I., Rada, L.: Solitary wave solutions to the tzitzeica type equations obtained by a new efficient approach. J. Appl. Anal. Comput. **9**, 568–589 (2019)
34. Zhang, R.F., Bilige, S.D., Fang, T., Chaolu, T.: New periodic wave, cross-kink wave and the interaction phenomenon for

the Jimbo–Miwa-like equation. Comput. Math. Appl. **78**, 754–764 (2019)
35. Ma, W.X.: Lump-type solutions to the (3+1)-dimensional Jimbo–Miwa equation. Int. J. Sci. Num. **17**, 355–359 (2017)
36. Wang, Y.H., Wang, H., Dong, H.H., Zhang, H.S., Temuer, C.: Interaction solutions for a reduced extended (3+1)-dimensional Jimbo–Miwa equation. Nonlinear Dyn. **92**, 487–497 (2018)
37. Zhang, R.F., Bilige, S.D.: New interaction phenomenon and the periodic lump wave for the Jimbo–Miwa equation. Mod. Phys. Lett. B **33**, 1950067 (2019)
38. Qi, F.H., Huang, Y.H., Wang, P.: Solitary-wave and new exact solutions for an extended (3+1)-dimensional Jimbo–Miwa-like equation. Appl. Math. Lett. **100**, 106004 (2020)
39. Guo, H.D., Xia, T.C., Hu, B.B.: High-order lumps, high-order breathers and hybrid solutions for an extended (3+1)-dimensional Jimbo–Miwa equation in fluid dynamics. Nonlinear Dyn. **100**, 601–614 (2020)
40. Kuo, C.K., Ghanbari, B.: Resonant multi-soliton solutions to new (3+1)-dimensional Jimbo–Miwa equations by applying the linear superposition principle. Nonlinear Dyn. **96**, 459–464 (2019)
41. Liu, J.G., Zhu, W.H., Osman, M.S., Ma, W.X.: An explicit plethora of different classes of interactive lump solutions for an extension form of 3d-Jimbo–Miwa model. Eur. Phys. J. Plus **135**, 412 (2020)
42. Ma, W.X.: Generalized bilinear differential equations. Stud. Nonlinear Sci. **2**(4), 140–144 (2011)
43. Hu, W.P., Deng, Z.C., Han, S.M., Zhang, W.R.: Generalized multi-symplectic integrators for a class of hamiltonian nonlinear wave pdes. J. Comput. Phys. **235**, 394–406 (2013)
44. Hu, W.P., Yu, L.J., Deng, Z.C.: Minimum control energy of spatial beam with assumed attitude adjustment target. Acta Mech. Solida Sin. **33**, 51–60 (2020)
45. Hu, W.P., Deng, Z.C., Wang, B., Ouyang, H.J.: Chaos in an embedded single-walled carbon nanotube. Nonlinear Dyn. **72**, 389–398 (2013)
46. Hu, W.P., Deng, Z.C.: Interaction effects of DNA, RNA-polymerase, and cellular fluid on the local dynamic behaviors of DNA*. Appl. Math. Mech. -Engl. Ed. **41**(4), 623–636 (2020)
47. Hu, W.P., Deng, Z.C.: Non-sphere perturbation on dynamic behaviors of spatial flexible damping beam. Acta Astronaut. **152**, 196–200 (2018)
48. Hu, W.P., Wang, Z., Zhao, Y.P., Deng, Z.C.: Symmetry breaking of infinite-dimensional dynamic system. Appl. Math. Lett. **103**, 106207 (2020)
49. Hu, W.P., Zhang, C.Z., Deng, Z.C.: Vibration and elastic wave propagation in spatial flexible damping panel attached to four special springs. Commun. Nonlinear Sci. Numer. Simulat. **84**, 105199 (2020)
50. Hu, W.P., Ye, J., Deng, Z.C.: Internal resonance of a flexible beam in a spatial tethered system. J. Sound Vib. **475**, 115286 (2020)